 

PACS numbers: 52.20.Hv; 52.50.Jm; 52.70.La
DOI: 10.1070/QE2007v037n11ABEH013608

# Charge exchange of multiply charged laser plasma ions with rare-gas jet atoms

I.L. Beigman, V.E. Levashov, K.N. Mednikov, A.S. Pirozhkov, E.N. Ragozin, I.Yu. Tolstikhina

***Abstract*. The interaction of a gas jet (He, Ne, Xe) with the incident laser plasma from a solid target [B, $(CH_2)_n$, $(CF_4)_n$] removed by $\sim 1$ cm is investigated. Line spectra arising from the charge exchange of multiply charged plasma ions with rare-gas atoms are recorded in the multiply charged ions – gas interaction region. The ratios between the partial cross sections of the charge exchange with the production of these ions in excited states are determined from the relative intensities of the Balmer series transitions in B V and C VI ions. These results are compared with theoretical data.**

***Keywords***: *charge exchange, multiply charged ions, partial cross sections, X-ray spectra.*

## 1. Introduction

In this paper we consider the charge exchange reactions of ions $X^{q+} + A \rightarrow X_{nl}^{*(q-1)+} + A^+$, where $X^{q+}$ is the incident multiply charged ion; A is a neutral atom; $X_{nl}^{*(q-1)+}$ is the ion produced in an excited state with the principle ($n$) and orbital ($l$) quantum numbers; and $A^+$ is the resultant singly charged ion. The interest in these processes is largely related to the facts that the ions produced in the excited state and the charge exchange cross section can be relatively high ($10^{-15} - 10^{-14}$ cm$^2$) – higher than for other processes involving multiply charged ions. In addition, the charge exchange is inherently quasi-resonant, which basically permits effecting selective population of multiply charged ion levels and may give rise to population inversion on their transitions in the soft X-ray range [1 – 3]. Experimental research has been carried out in this direction and is currently underway [4, 5].

The charge exchange cross section has repeatedly been measured in ion-beam experiments; however, the distribution of reaction products over the energy levels remains unknown in this case. This distribution can be found by observing the transitions of multiply charged ions in the soft X-ray range. In the sparse experimental works in this area, the charge exchange reactions are associated with the emergence of individual spectral lines in the plasma or with an increase in their intensity, which, however, can be caused by other processes as well (electron – ion recombination or additional plasma heating). The 10.2-nm $H_\alpha$ line of the O VIII ion was observed in the tokamak plasma [6] upon the injection of a beam of neutral hydrogen atoms. The authors attributed the population of the $n = 3$ level to the reaction of charge exchange of oxygen nuclei with hydrogen atoms:

$$O^{8+} + H \rightarrow O^{*7+} + H^+.$$

However, it was noted that the corresponding intensity increase in $Ly_\alpha$ and $Ly_\beta$ lines (the $2 \rightarrow 1$ and $3 \rightarrow 1$ transitions) was not observed. In a more complex system, like a laser plasma expanding into a buffer gas, the role of charge exchange was demonstrated by comparing experimental spectra with numerical simulations [4]. In Ref. [5], the carbon plasma produced by irradiating a 6-mm long and 20-μm wide strip on a plane carbon target by a laser pulse (1.5 ps, 10 J, $5 \times 10^{15}$ W cm$^{-2}$), which consisted primarily of bare $C^{6+}$ nuclei, expanded into a jet of He atoms produced by a pulsed valve. Theoretical calculations based on a collisional-radiative model and preliminary experiments [5] demonstrate the presence of inversion and amplification on the $H_\alpha$ transition ($3 \rightarrow 2$, $\lambda = 18.2$ nm) of hydrogen-like C VI ions. The charge exchange of $C^{4+}$ ions with hydrogen atoms was observed using the lines arising from transitions in the vacuum UV spectral range in Ref. [7].

It was assumed in [8] that the relatively recently discovered soft X-rays from comets are produced due to the charge exchange of multiply charged solar wind ions with the components of the cometary tail. Ion-beam measurements of the cross sections for the charge exchange of C, N, O, and Ne ions with the molecules $CO_2$, $H_2O$, and $H_2$, and He atoms were performed [9].

As in our earlier experiments [10], we investigated the charge exchange of multiply charged ions of a laser plasma, produced by irradiation of a solid target with the neutral atoms of a rare-gas jet in vacuum. The characteristic ion energies ($\sim 1$ keV nucleon$^{-1}$) were due to the expansion dynamics of the laser plasma. We observed the charge exchange by recording spatially resolved soft X-ray spectra arising due to the radiative decay of the excited $X_{nl}^{*(q-1)+}$ ion states. The simultaneous recording of several spectral lines gives information on the charge exchange product distribution over the energy levels with different $n$, i.e. eventually on the ratios of the partial cross sections for the charge exchange.

**I.L. Beigman, V.E. Levashov, K.N. Mednikov, A.S. Pirozhkov, E.N. Ragozin, I.Yu. Tolstikhin** P.N. Lebedev Physics Institute, Russian Academy of Sciences, Leninsky prosp. 53, 119991 Moscow, Russia; e-mail: enragozin@sci.lebedev.ru

Received 24 April 2007
*Kvantovaya Elektronika* **37** (11) 1060 – 1064 (2007)
Translated by E.N. Ragozin

## 2. Experimental

Experiments were performed in a IKAR large vacuum chamber (∅0.9 m × 3.8 m) by using a 1.08-μm $Nd:YAlO_3$ laser emitting 6-ns, 0.5-J pulses, which was located near the chamber end flange. The stream of the laser plasma produced by irradiating a solid target by the nanosecond pulses of the neodymium laser was directed to a gas jet. The gas jet was produced with a high-pressure pulsed gas valve, whose actuation was timed with the laser shot. Both a cylindrical nozzle 0.4 mm in diameter and a conical nozzle in the form of a 1-cm long channel with an outlet 1.0 mm in diameter for an outlet–inlet area ratio $S_{out}/S_{in} \approx 5.0$. The gas was delivered to the valve from high-pressure vessels. The valve was opened for $\sim 1.5$ ms. The density distribution in the jet for the nozzles of both types was investigated earlier in [11], where the expansion of xenon atoms was simulated and the density distribution was measured by the absorption of the 13.5-nm radiation in the jet. For donor atoms, in different experiments we employed atoms of He, Ne, and Xe.

The jet axis was parallel to the solid target and was separated from it by a distance of 11 mm (Fig. 1). The laser beam was focused onto the target to a spot with an effective area $S_{eff} \sim 10^{-5}$ cm$^2$ using a lens with a focal distance $f =$ 75 mm made of a heavy flint glass. The maximum intensity of laser radiation at the centre of the focal spot was no less than $5 \times 10^{12}$ W cm$^{-2}$.

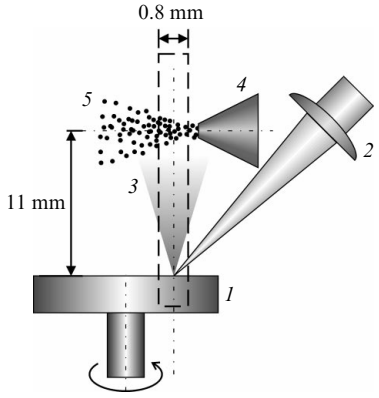


**Figure 1.** Relative position of the laser plasma (*3*) and the gas cloud (*5*): (*1*) rotary target; (*2*) lens for laser radiation focusing; (*4*) nozzle of the pulsed gas valve; dashed lines show the field of view of the spectrograph.

Spectra were recorded with the spatial resolution by using a high-transmission broadband spectrograph comprising a normal-incidence aperiodic multilayer (Mo/Si) mirror with an almost uniform reflectivity throughout the 12.5–25 nm range and a wide-aperture free-standing transmission diffraction grating (1000 or 5000 lines mm$^{-1}$) (Fig. 2) [12–14]. The spectrograph possessed the following combination of properties: stigmatism, a vertical field of view of $\sim 2$ cm, a spectral resolving power of no less than 300, a broad operating spectral range, and a record-high transmission. Owing to the large dimension ($\sim 2$ cm) of the vertical field of view, we recorded the radiation both from the hot plasma at the surface of the solid target and from the plasma–gas interaction region, which yielded the spatial picture of the interaction. The distance between the axis of the plasma cone and the entrance slit of the spectrograph was 16 mm. Considering the spectrograph acceptance angle, the radiation was recorded from the region 0.8 mm in width. This region is indicated by dashed lines in Fig. 1. The short-wavelength bound (12.5 nm) of the spectrograph operating range was determined by the Si L-edge absorption, whereas the long-wavelength bound was absent in fact. When a magnesium target was irradiated, we observed the $1s^2\,2s\,^2S_{1/2} - 1s^2\,2p\,^2P_{3/2,1/2}$ doublet in the Mg X ion at 60.989 and 62.495 nm.

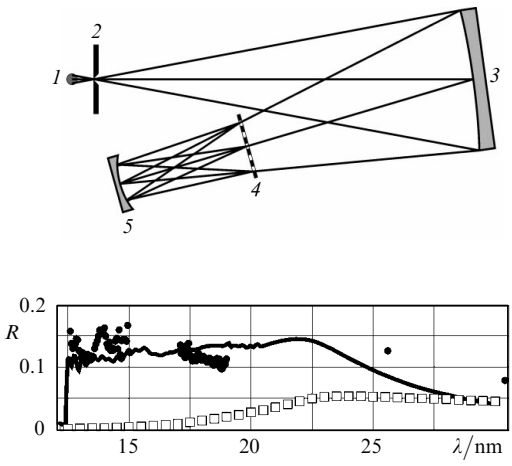


**Figure 2.** Scheme of the spectrograph [(*1*) laser-produced plasma under investigation; (*2*) entrance slit; (*3*) aperiodic normal-incidence multilayer (Mo/Si) mirror with an aperture of 50 mm and a radius of curvature of 1 m; (*4*) free-standing transmission diffraction grating (1000 or 5000 lines mm$^{-1}$); (*5*) film holder with UF-4 X-ray photographic film), as well as the wavelength dependence of multilayer mirror reflectivity (solid curve is calculation, full circles are data of measurements performed at the Institute for the Physics of Microstructures, RAS, squares are reflectivity of bulk molybdenum (for comparison)].

The spectra were recorded on a UF-4 X-ray photographic film, which provides a spatial resolution of at least 160 lines mm$^{-1}$. The photospectrograms were digitised with an Epson Perfection 4870 scanner with an optical resolution of 4800 lines per inch, a calibrated step attenuator being scanned simultaneously with the photospectrograms to obtain the absolute photographic-film blackening. Figure 3 shows a spectrogram recorded in the irradiation of a boron target, with helium used as the donor atom.

Teflon $(CF4)_n$, polyethylene, and boron discs were employed as targets. For the boron target we used sintered crystalline boron tablets (99 % B, 1 % C) $\sim 30$ mm in

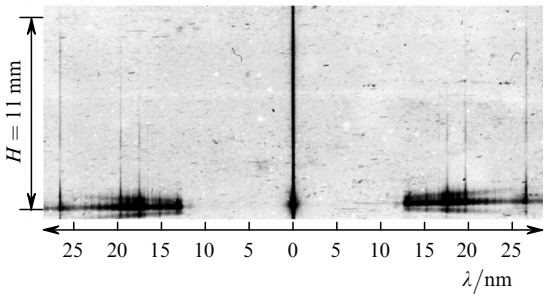


**Figure 3.** Panoramic spectrum recorded upon interaction of the boron target plasma with a supersonic helium jet; *H* is the distance to the target.

diameter, the tablet surface to be irradiated was ground on an optical abrasive disc.

As indicated above, the field of view of the spectrograph encompassed both the target surface and the plasma–gas interaction region. The spectrum of plasma at the target surface contained ionic lines belonging to the ions C IV–C VI and B III–B V. At a distance of several millimetres from the target, the spectral line intensities of multiply charged ions strongly decreased compared to their intensity near the surface of the solid target, and the lines were hardly visible. However, in the plasma–gas interaction region in all experiments we observed the recovery of emission at several spectral lines. We attribute this experimental fact to an intense population of excited states of the plasma ions in their charge exchange with neutral gas atoms. Figure 4 shows the intensities of the Balmer lines of the B V ion as functions of the distance to the solid target. One can see that the levels of B V are actively populated due to the charge exchange even at a distance of $\sim 3$ mm from the jet axis, where the density of the donor atoms is $10^{15} - 10^{16}$ cm$^{-3}$. The wavelengths of the first three transitions of the Balmer series ($n \to 2$) of, for instance, the B V ion are equal to 26.24 nm ($H_\alpha$), 19.44 nm ($H_\beta$), and 17.35 nm ($H_\gamma$).

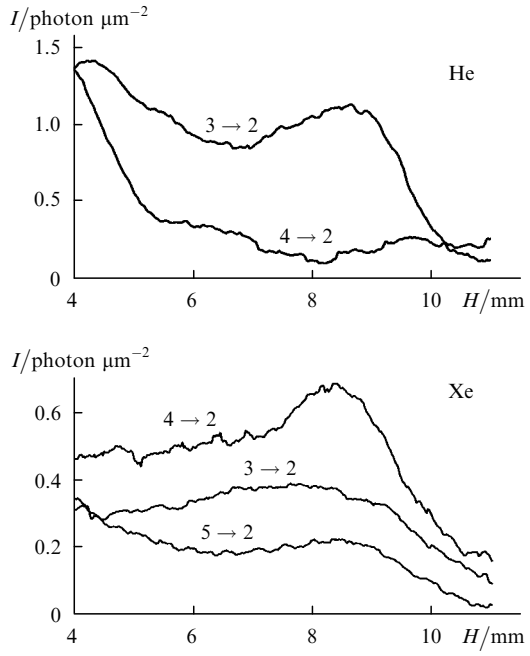


**Figure 4.** Intensities of B V ion lines as functions of the distance $H$ to the target upon interaction of the B VI ions with He and Xe atomic beams for the transitions $3 \to 2$ ($\lambda = 26.24$ nm), $4 \to 2$ ($\lambda = 19.44$ nm), and $5 \to 2$ ($\lambda = 17.35$ nm).

Unlike papers [4, 5], in our experiment the plasma and the jet of donor atoms are formed separately. The distance between the solid target and the jet axis was selected so that the electron density of the plasma stream in the interaction region did not exceed $10^{16}$ cm$^{-3}$. In this case, the hydrogen-like levels of the C VI and B V ions populated by charge exchange were in the 'radiative domain' (see below), making it possible to interpret the relative line intensities of the Balmer series in terms of partial charge-exchange cross sections.

## 3. Measurement data

First of all we emphasise that the interpretation of the experimental data is substantially simpler when the levels populated in the charge exchange are located in the 'radiative domain' in the sense that the condition

$$N_e < N_e^{(p)} = \frac{A(p)}{c(p, p \mp 1)} \tag{1}$$

is fulfilled, where $N_e$ is the electron density; $A(p)$ is the total radiative decay probability of the $p$th level; and $c(p, p \mp 1)$ is the collisional (de)excitation rate of the level. When $N_e = N_e^{(p)}$, the $p$th level is said to be at the boundary between the radiative and collisional domains. When inequality (1) is fulfilled, almost every event of population of levels with $n \leqslant p$ is accompanied by cascade downward radiative transitions, while collisions have no effect on the relative line intensities. For hydrogen-like ions, condition (1) may be formulated in an analytical form:

$$N_e < N_e^{(p)} = 1.7 \times 10^{17} Z^7 \tau(p) p^{-9.3} \text{ cm}^{-3}, \tag{2}$$

where $\tau(p) \approx 3 \ln p - 0.247$ and $Z$ is the nuclear charge. Below, we will discuss with the levels $n \leqslant 5$ of the hydrogen-like C VI and B V ions populated in the charge exchange of carbon and boron nuclei. For these levels, conditions (1) and (2) are fulfilled when Ne is lower than $7 \times 10^{16}$ cm$^{-3}$ (C VI) and $2 \times 10^{16}$ cm$^{-3}$ (B V). In our experiment, the plasma–gas interaction begins to clearly manifest itself at a distance of about 8 mm from the solid target, where the maximum electron density is $(1 - 3) \times 10^{15}$ cm$^{-3}$. Therefore, the relative line intensities are unaffected by collisions with electrons.

Let us denote by $\sigma_n$ the partial cross sections for charge exchange into level $n$ of a hydrogen-like ion. Then, the intensity $I_n$ (the number of emitted photons) of the lines of the Balmer corresponding to the $n \to 2$ ($n \leqslant n_{\max}$) radiative transitions is

$$I_n \propto \frac{A(n,2)}{A(n)} \sum_{n'=n}^{n_{\max}} v \sigma_{n'} C(n', n), \tag{3}$$

where $n_{\max}$ is the principal quantum number of the highest level populated by the charge exchange; $C(n', n)$ is an element of the cascade Seaton matrix, which determines the probability that an atom initially excited to level $n'$ finds itself in level $n$ due to one or several radiative transitions [15]; $A(n, 2)$ is the radiative $n \to 2$ transition probability; and $v$ is the relative velocity of the multiply charged ion and the rare-gas atom. When only the levels with $n \leqslant 4$ are populated we have

$$\frac{\sigma_3}{\sigma_4} = \frac{I_3}{I_4} \frac{A(3)A(4,2)}{A(4)A(3,2)} - C(4,3) = 0.63 \frac{I_3}{I_4} - 0.30. \tag{4}$$

Upon the population of levels with $n \leqslant 5$, we obtain

$$\begin{aligned} \frac{\sigma_4}{\sigma_5} &= \frac{I_4}{I_5} \frac{A(4)A(5,2)}{A(5)A(4,2)} - C(5,4) = 0.78 \frac{I_4}{I_5} - 0.23, \\ \frac{\sigma_3}{\sigma_5} &= \frac{I_3}{I_5} \frac{A(3)A(5,2)}{A(5)A(3,2)} - C(5,3) - \frac{I_4}{I_5} \frac{A(4)A(5,2)}{A(5)A(4,2)} C(4,3) \\ &\quad + C(5,4)C(4,3) = 0.50 \frac{I_3}{I_5} - 0.23 \frac{I_4}{I_5} - 0.19. \end{aligned} \tag{5}$$

Note that it follows from expressions (4) and (5) that $I_3/I_4 > 0.5$ and $I_4/I_5 > 0.3$.

The entire Balmer series of the ion B V falls into the operating spectral range of the spectrograph. Upon the charge exchange of boron nuclei with He atoms with the ground level lying 3.3 eV below the level with $n = 4$, we observed the $H_\alpha$ and $H_\beta$ lines, the $H_\alpha$ line being approximately six times stronger, which corresponds to a partial cross section ratio $\sigma_3/\sigma_4 = 3.5$. Upon the charge exchange of boron nuclei with Ne atoms, whose ground level is 0.3 eV below the $n = 4$ level, the $H_\alpha$ and $H_\beta$ lines are also observed, but the relative intensity of the $H_\beta$ line in this case is two times higher than in the case with He, corresponding to a ratio $\sigma_3/\sigma_4 = 1.5$. Upon the charge exchange of boron nuclei with Xe atoms, whose ground level lies 1.5 eV above the level with $n = 5$, we observed the lines $H_\alpha$, $H_\beta$, and $H_\gamma$ (with an intensity ratio of 1.9 : 2.9 : 1), with $\sigma_3 : \sigma_4 : \sigma_5 = 0.05 : 2.1 : 1$. These observations confirm the qualitative theoretical predictions that one–two levels which lie below the ground level of the donor atom (or close to it) should be populated strongest in the charge exchange (Fig. 5). Furthermore, the absence of the Balmer lines originating from the levels with $n > 5$ in the case of Xe and from the levels with $n > 4$ in the cases of He and Ne means that other (recombination) mechanisms do not make an appreciable contribution to the population of the excited states. The 'centre of gravity' of the distribution of partial cross sections shifts towards higher levels with decreasing ionisation potential of the donor atom, which is reflected in Fig. 6. The experimental data correlate with the theoretical calculations of the cross sections (Table 1).

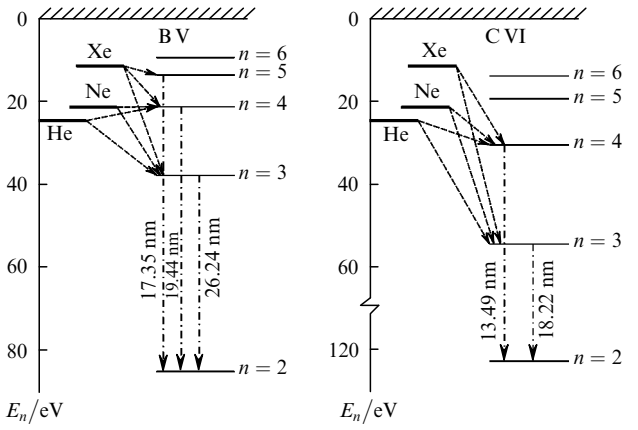


**Figure 5.** Energy level diagrams of the B V and C VI ions and energy levels of the ground states of rare-gas atoms. The dashed arrows indicate the experimentally observed electron transitions from a donor atom to a multiply charge ion and dot-and-dash lines indicate the radiative transitions in the ions.

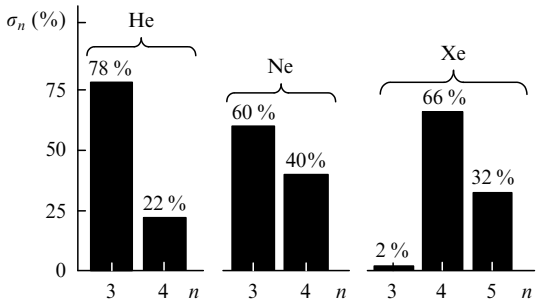


**Figure 6.** Partial cross sections for the charge exchange of boron nuclei with neutral rare-gas atoms.

In the case of carbon, the operating spectral range encompassed the lines $H_\alpha$ and $H_\beta$. Upon the charge exchange of carbon nuclei with Ne atoms, whose ground level lies 9 eV above the level with $n = 4$ and 2 eV below the level with $n = 5$, we observed the lines $H_\alpha$ and $H_\beta$ (Fig. 5). In this case, as shown by a comparison with the data on boron, it is not unlikely that we overlook the relatively weak channel of $n = 5$ level population, which would give rise to the $H_\gamma$ line. Upon the charge exchange of carbon nuclei with He atoms, whose ground level lies 6 eV above the $n = 4$ level and 5 eV below the $n = 5$ level, we also observed both lines ($H_\alpha$ and $H_\beta$). In this case, the relative intensity of the $H_\alpha$ line is 2.5 times higher (in comparison with the charge exchange with neon atoms).

We performed theoretical calculations of charge exchange cross sections using the ARSENY code [16] elaborated by E.A. Solov'ev during the period from 1986 to 1992 and used to calculate the cross sections for different processes in slow ion–atom collisions [17–21] in the range of collision energies $E$ up to 10 keV nucleon$^{-1}$. The theoretical method employed in the ARSENY code relies on the effect of hidden crossing of quasimolecular energy levels, which was discovered in Ref. [22]. The efficiency of the hidden crossing method in atomic physics has been confirmed in several international conferences on the physics of electron and atomic collisions (see, for instance, Ref. [23]). It is pertinent to note that the ARSENY code is intended for the calculation of reaction cross sections in a system consisting of two Coulomb centres and one electron. Introducing the effective charge $Z_{\text{eff}}$ by the relation

$$\frac{Z_{\text{eff}}\text{Ry}}{n^2} = I,$$

where $I$ and $n$ are the ionisation potential and the principal quantum number of the active electron of a rare-gas atom, enables using this code for the investigation of collisions of multielectron systems.

**Table 1.** Calculated and measured cross section ($\sigma_3/\sigma_4$) and intensity ($I_3/I_4$) ratios.

| Reaction | $\sigma_3/\sigma_4$ | | | $I_3/I_4$ | | |
|---|---|---|---|---|---|---|
| | Calculation | | Experiment | Calculation | | Experiment |
| | $E = 1$ keV nucleon$^{-1}$ | $E = 2$ keV nucleon$^{-1}$ | | $E = 1$ keV nucleon$^{-1}$ | $E = 2$ keV nucleon$^{-1}$ | |
| $B^{5+} + He$ | 16.5 | 19 | $3.5^{+1.9}_{-1.3}$ | 26.6 | 30.6 | $6^{+3}_{-2}$ |
| $B^{5+} + Ne$ | 1.94 | 1.87 | $1.5^{+0.7}_{-0.7}$ | 3.55 | 3.44 | $2.9^{+1.1}_{-1.1}$ |
| $C^{6+} + He$ | 0.96 | 1.77 | $1.7^{+0.7}_{-0.7}$ | 2.0 | 3.3 | $3^{+1.3}_{-1}$ |
| $C^{6+} + Ne$ | 0.012 | 0.024 | $0.45^{+0.4}_{-0.06}$ | 0.5 | 0.51 | $1.2^{+0.6}_{-0.1}$ |

The cross section ratios $\sigma_3/\sigma_4$ and intensity ratios $I_3/I_4$ for several charge exchange reactions, which were obtained by calculations and in experiments, are collected in Table 1. According to the calculations, at low collision velocities in all cases there practically occurs population of one – two levels of a hydrogen-like ion, which lie several electronvolts below the ground level of the donor atom. This is also confirmed by the experiment: upon the charge exchange of boron nuclei with He and Ne atoms, the $5 \rightarrow 2$ transition line is hardly visible and its intensity defies evaluation.

In the case of the reactions $B^{5+} + Ne$ and $C^{6+} + He$ (the 2nd and 3rd lines in Table 1) the theory agrees quantitatively with the experiment. In the other two cases (the 1st and 4th lines), only qualitative agreement exists.

According to the theoretical calculations, upon the charge exchange of carbon nuclei with He atoms, the calculated ratio $\sigma_3/\sigma_4$ essentially depends on the particle collision energy (Fig. 7). In this case, the experimental ratio $\sigma_3/\sigma_4 = 1.7$ is characteristic for the velocities of colliding nuclei and He atoms of $\sim 5.7 \times 10^7$ cm s$^{-1}$. For expansion velocities typical of laser-produced plasmas, the partial cross section for the charge exchange (with He atoms) for the level $n = 5$ of C VI ions is less than 0.5 % of the total cross section.

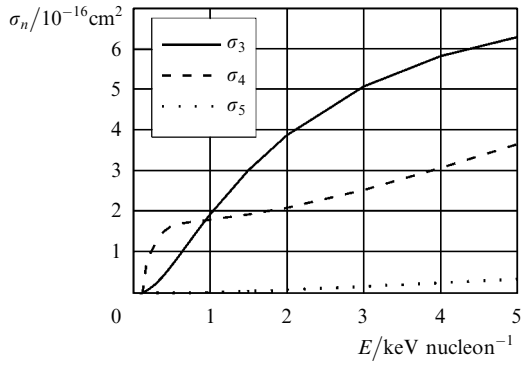


**Figure 7.** Partial charge exchange cross sections for the 3 – 5 levels of hydrogen-like C VI ions upon collisions of carbon nuclei with He atoms calculated as functions of the collision energy. The excitation cross sections for the remaining levels are negligible.

Table 2 shows the partial cross section and intensity ratios in the one-electron charge exchange of boron atoms with xenon atoms determined from the relative intensities of the Balmer lines of B V ions. Figure 6 shows how the charge exchange partial cross section distribution over the B V ion levels changes under replacement of the donor gas. The distribution 'centre of gravity' shifts towards higher $n$ on lowering the ionisation potential of the donor gas.

**Table 2.** Partial cross section and intensity ratios measured in the charge exchange of boron nuclei with Xe atoms.

| Reaction | $\sigma_3/\sigma_4$ | $\sigma_4/\sigma_5$ | $I_3/I_4$ | $I_4/I_5$ |
|---|---|---|---|---|
| $B^{5+} + Xe$ | $0.025^{+0.15}_{-0.025}$ | $2^{+0.9}_{-0.3}$ | $0.64^{+0.2}_{-0.2}$ | $2.9^{+1.1}_{-0.4}$ |

## 4. Conclusions

In the region of interaction between a rarefied laser plasma and a rare-gas (He, Ne, Xe) jet, we have observed the Balmer series lines ($H_\alpha$, $H_\beta$, $H_\gamma$) of the hydrogen-like C VI and B V ions arising from charge exchange. Several qualitative features of the observed spectra are unambiguously indicative of the charge exchange as the principal mechanism of level population. These features are the absence of higher members of the series, the change of the highest observable series member in accordance with the change of ionisation potential of the gas atoms, as well as the shifting of the 'centre of gravity' of the $\sigma_n$ distributions towards higher $n$ on lowering the ionisation potential of the gas atoms. From the relative intensities of the Balmer series lines we determined the charge exchange cross section ratios for the $n = 3$, 4 levels of C VI and B V ions and for the $n = 5$ levels in the interaction of boron nuclei with Xe.

For the charge exchange reactions $B^{5+} + Ne$ and $C^{6+} + He$, the experimental $\sigma_3/\sigma_4$ ratios are qualitatively consistent with the theoretical data.

***Acknowledgements.*** The authors thank E.A. Solov'ev for placing at our disposal the ARSENY code and P.V. Sasorov for helpful discussions. This work was supported by the Russian Foundation for Basic Research (Grant Nos 04-02-16209, 05-02-16658, 06-02-16298, 07-02-00316) and the 'Optical Spectroscopy and Frequency Standards' Basic Research Programme of the Physical Sciences Division, Russian Academy of Sciences.

## References

1. Presnyakov L.P., Shevel'ko V.P. *Pis'ma Zh. Eksp. Teor. Fiz.*, **13**, 286 (1971).
2. Vinogradov A.V., Sobel'man I.I. *Zh. Eksp. Teor. Fiz.*, **63**, 2113 (1972).
3. Presnyakov L.P., Ulantsev A.D. *Kvantovaya Elektron.*, **1**, 2377 (1974) [*Sov. J. Quantum Electron.*, **4**, 1320 (1974)].
4. Dixon R.H., Seely J.F., Elton R.C. *Phys. Rev. Lett.*, **40** (2), 122 (1977).
5. Kawachi T., Kado M., Tanaka M., Hasegawa N., Nagashima A., Kato Y. *J. Phys. IV*, **11**, Pr.2-255 (2001).
6. Isler R.C. *Phys. Rev. Lett.*, **38** (23), 1359 (1977).
7. Vorontsov V.A., Born M., Shaikhislamov I.F., et al. *J. Phys. B: At. Mol. Opt. Phys.*, **36**, 3865 (2003).
8. Cravens T.E. *Geophys. Res. Lett.*, **24**, 105 (1997).
9. Greenwood J.B., Williams I.D., Smith S.J., Chutjian A. *Astrophys. J.*, **533**, L175 (2000); *Phys. Rev. A*, **63**, 062707 (2001).
10. Levashov V.E., Mednikov K.N., et al. *Fiz. Plazmy*, **30** (2), 169 (2004) [*Plasma Phys. Reports*, **30** (2), 149 (2004)].
11. Boldarev A.S., Gasilov V.A., Levashov V.E., Mednikov K.N., Pirozhkov A.S., Pirozhkova M.S., Ragozin E.N. *Kvantovaya Elektron.*, **34**, 679 (2004) [*Quantum Electron.*, **34**, 679 (2004)].
12. Kondratenko V.V., Levashov V.E., Pershin Yu.P., Pirozhkov A.S., Ragozin E.N. *Kratk. Soobshch. Fiz.*, (7), 32 (2001).
13. Beigman I.L., Pirozhkov A.S., Ragozin E.N. *Pis'ma Zh. Eksp. Teor. Fiz.*, **74**, 167 (2001) [*JETP Lett.*, **74** (3), 149 (2001)].
14. Ragozin E.N., Kondratenko V.V., Levashov V.E., Pershin Yu.P., Pirozhkov A.S. *Proc. SPIE Int. Soc. Opt. Eng.*, **4782**, 176 (2002).
15. Vainshtein L.A., Sobel'man I.I., Yukov E.A. *Excitation of Atoms and Broadening of Spectral Lines* (Springer – Verlag: Berlin, Heidelberg, New York, 1995).
16. Solov'ev E.A. *Proc. XIX ICPEAC* (Whistler, Canada). Ed. by L.J. Dube et al. (New York: AIP Press, 1995) p. 471.
17. Grozdanov T.P., Solov'ev E.A. *Phys. Rev. A*, **38**, 4333 (1988).
18. Janev R.K. et al. *Phys. Rev. A*, **49**, R645 (1994).
19. Janev R.K., Solov'ev E.A., Wang Yi. *J. Phys. B*, **29**, 2497 (1996).
20. Janev R.K., Solov'ev E.A., Ivanovski G. *Phys. Scripta T*, **62**, 43 (1996).
21. Janev R.K., Solov'ev E.A. *J. Phys. B*, **30**, L353 (1997).
22. Solov'ev E.A. *Usp. Fiz. Nauk.*, **157** (3), 437 (1989).
23. Solov'ev E.A. *Proc. XX Int. Conf. on the Physics of Electronic and Atomic Collisions (ICPEAC)* (Vienna, Austria, 1997).